2010 13th International IEEE
Annual Conference on Intelligent Transportation Systems
Madeira Island, Portugal, September 19-22, 2010

Fast lane detection & tracking based on Hough transform with reduced memory requirement

Jung Gap Kuk†, Jae Hyun An†, Hoyong Ki‡ and Nam Ik Cho†
†Department of Electrical and Computer Engineering,Seoul National University, Seoul, Korea
‡Automation and Systems Research Institute, WISE automotive Corporation, Seoul, Korea
e-mail: jg-kuk@ispl.snu.ac.kr, jhahn@ispl.snu.ac.kr, khy@wise-automotive.com and nicho@snu.ac.kr

Abstract— **In this paper, we present a computationally efficient and robust lane detection algorithm based on Hough transform. The proposed method first extracts lane markings by applying 1D ridge detector to each row of an image. Given the extracted ridge points, the lane is then detected by applying Hough transform. Unlike the conventional methods, we consider only small set of line candidates which pass through a circle centered at previously detected vanishing point. The set is quite small and it is represented by a small region on a parametric domain. Hence, the proposed method needs much smaller accumulation array than conventional one and reduces the required memory. In addition, we propose modified parametric domain which encodes approximated lateral positions and the current lateral positions are searched on the modified parametric domain within certain region centered at previously detected positions. This proposed tracking scheme on the parametric domain considers temporal coherency and enables robust detection even when actual lane is weakly represented on the parametric domain. Experimental results show that the proposed method robustly detects the lane with reduced memory requirement.**

I. Introduction

The intelligent vehicle system has been a topic of great interest for decades. One of the most important goals of the system is to achieve a safer driving environment by automatically analyzing the circumstances surrounding the vehicle and giving a driver warning or some information. For the system, obstacle may be detected to avoid impending collision [1] and the distance of a vehicle from the lane boundary may be calculated to avoid the unaware lane departure. In these applications, the first step is to detect the lanes by image processing and numerous methods have been developed on this issue. Many of these works assume that the lane is represented by a straight line in the nearest field (lower part in an image) and Hough transform is chosen to robustly detect the lane [2]–[4]. On the other hand, the lane is modeled by a hyperbola-pair model and RANSAC (RANdom SAmple Consensus) is applied to estimate the model parameter [5]. The lane can also be modeled by cubic spline, and RANSAC and particle filtering are used for the estimation of the lane parameters [6]. Theoretically, the extrinsic and intrinsic camera parameters explain the projection from 3D world to 2D image and thus some of other methods incorporate the camera parameter estimation and the lane detection into an integrated framework. This approach is mostly based on probabilistic scheme such as Kalman filtering [7] and particle filtering [8]. Although above methods show good performance even when dealing with challenging scenarios, the algorithms are too complicated to be implemented on a cheap DSP. Hence in this paper, we propose a computationally efficient and robust lane detection algorithm based on hough transform.

A. Overview of the Proposed Algorithm

The proposed algorithm can be roughly divided into two steps : lane marking extraction and lane detection based on Hough transform. In the lane marking extraction step, the lane marking is assumed to be a ridge and lane markings are extracted by applying 1D ridge detector to each row of an image. In the next step, the lane is detected based on Hough transform given the extracted ridge points. Unlike the conventional methods, the proposed method considers only small set of line candidates which pass through a circle centered at previously detected vanishing point. This is based on the observation that currently detected vanishing point is to be close to previously detected vanishing point. The size of the set is quite small and the set is represented by a small region in the parametric domain. We call this region ROIPD (Region Of Interest in Parametric Domain). Hence, the proposed method needs much smaller accumulation array than conventional one and also reduces the computational complexity because computations for the lines except for the line candidates are not performed. In addition, we propose modified parametric domain which encodes approximated lateral positions of the lane and the current lateral positions of the lanes are searched on the modified parametric domain within certain range centered at previously detected lateral positions. With this lane tracking scheme, the lateral positions are robustly detected even when actual lane is weakly represented on the parametric domain. To sum up in this step, the spatial positions of extracted ridge points are first transformed to ROIPD and the current lateral positions are searched on ROIPD within certain region centered at the previous lateral positions.

The rest of paper is organized as follows: Hough transform is briefly reviewed in Section II and details of the proposed method are explained in Section III. First ridge points are extracted in Section III-A and two key components of the proposed algorithm, the memory reduction method and the modified parametric domain, are explained in Section III-

978-1-4244-7659-6/10/$26.00 ©2010 IEEE

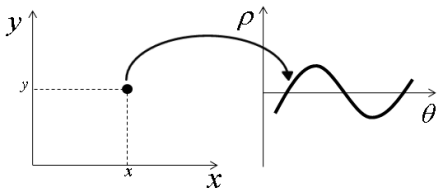

Fig. 1. Illustration of Hough transform.

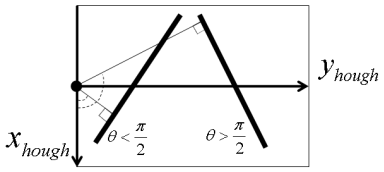

Fig. 2. The preferred coordinate system for Hough transform.

B and Section III-C respectively. Combining the results in Section III-A, III-B and III-C, we design the overall lane detection system with some implementation issue in Section III-D and show experimental results in Section IV. Finally conclusions are given in Section V.

II. Review of Hough Transform

Let $\mathbf{x} = (x, y)$ be a point detected by an edge detector. For the extraction of lines or line segments, Hough transform converts $\mathbf{x}$ to a curve $\rho - x\cos\theta - y\sin\theta = 0$ in the parametric domain $\mathbf{\Theta} = (\rho, \theta)$ where ρ denotes distance from a pre-defined origin to $\mathbf{x}$, and θ denotes the angle between two vectors $\vec{x} = (x, y)$ and $\vec{e} = (1, 0)$. An illustration of Hough transform is shown in Fig. 1. Based on the Hough transform, a line passing through collinear points is detected by finding an intersection of corresponding curves on the parametric domain. However in practical case, the points are hardly collinear but scattered around the line and thus curves do not exactly meet at one point. Hence the maximally intersected point is selected, instead. For the implementation, the parametric domain is generally represented by an accumulation array and each bin counts the number of points on the corresponding line.

It is worth noting that a location of an origin for Hough transform plays an important role in the case of lane detection because it affects the way of distinguishing between the left lane and the right lane. Throughout the paper, the origin for Hough transform will be called the Hough origin. If the Hough origin is located somewhere at the bottom of image, two planes are produced by vertical line passing the Hough origin and both of left and right lanes can appear on the same plane when a vehicle is changing the lane. Hence there can be some ambiguity in distinguishing between the left lane and the right lane. To avoid this ambiguity, the Hough origin should be located on the left side of the image as shown in Fig. 2. Based on this coordinate system, the lane changing occurs when $\theta = \pi/2$ and thus the left lane is sure to exist on the plane where $\theta < \pi/2$ and the right lane on the plane where $\theta > \pi/2$ as shown in Fig. 2.

III. Proposed Method

A. Lane Marking Extraction

To extract lane markings, most of algorithms detect edges based on image gradient. However the edge based technique is vulnerable to spurious lines due to pedestrian crossings, shadows, indicators and so on. Hence in our lane detection system, a ridge ($dark$-$bright$-$dark$) pattern is detected instead of the edge. A conventional way of extracting the ridge is to analyze 2D features such as eigenvalues of Hessian matrix in linear scale space [9] or minimum and maximum filter responses to second order Gaussian steerable filter designed to match the ridge [10], [11]. Fortunately, as the lane is aligned almost vertically in the near field, the ridge characteristic can still be found at each row of the image. Hence, we use the 1D ridge detector instead of 2D ridge detector.

Let us define the ridge descriptor $\mathbf{r}$ as a four dimensional vector $(x_c, \Delta_r, \Delta_f, l)$ where x_c denotes center position of the ridge, Δ_r and Δ_f denote strengths of rising edge and falling edge respectively and l denotes ridge width. Note that the strength of edge is measured by filtering the intensity image with first order derivative of Gaussian. With this definition, the ridge is extracted by evaluating saliency, polarity and scale defined as

$$\begin{aligned} \text{saliency} &: \min(\Delta_r, \Delta_f) > T_s \\ \text{polarity} &: \text{sign}(\Delta_r) > 0 \text{ and } \text{sign}(\Delta_f) < 0 \\ \text{scale} &: l < T_c \end{aligned}$$

where the saliency implies that both rising and falling edges should be sufficiently noticeable and the polarity explains that a lane is specified by dark-bright-dark pattern, $i.e.$, convex. The condition for the scale is straightforward because lane width is within a certain range.

B. Reducing the Required Memory

In this section we propose to reduce the required memory when utilizing Hough transform. It is noted that the size of memory in Hough transform is determined by the range of parameters (the range of ρ is determined by image size and the range of θ by the location of the Hough origin) and the resolution of them. Given the assumption that the Hough origin is located at the center of left side of an image, we have the range of ρ by $0 \le \rho \le \rho_{\max}$ where $\rho_{\max}$ is maximum distance from the Hough origin as shown in Fig. 3 and the range of θ by $0 \le \theta \le \pi$. If quantization steps for the parameters ρ and θ are denoted as q_ρ and q_θ respectively, total memory size becomes $\lceil \rho_{\max}/q_\rho \rceil \times \lceil \pi/q_\theta \rceil$. Hence the general way of reducing the size of the accumulation array has been to raise the quantization steps, that is, lower the resolution of the parameters. In this paper, we reduce the size of accumulation array without the degradation of resolution, by confining the range of ρ to a small region of interest in the vicinity of vanishing point.

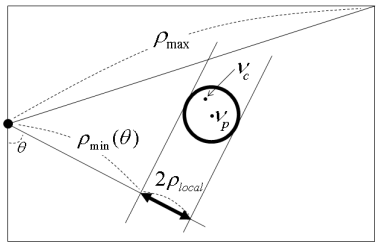

Fig. 3. The range of ρ.

Any parallel lines on a road including the lanes are to meet at a point which is called a vanishing point. Let the vanishing point in the previous frame be $\nu_{\mathbf{p}} = (\nu_x, \nu_y)$ and the current vanishing point $\nu_{\mathbf{c}}$. With the observation of slowly varying vanishing point, we may define a region of $\nu_{\mathbf{c}}$ as

$$|\nu_{\mathbf{c}} - \nu_{\mathbf{p}}| \leq \rho_{local} \tag{1}$$

which is illustrated in Fig. 3. This implies that among all possible lines, only the lines passing through the circle of radius ρ_{local} are the candidates for the lane. That is, ρ of line candidates satisfy

$$\rho_{\min}(\theta) \leq \rho(\theta) \leq \rho_{\min}(\theta) + 2\rho_{local}, \tag{2}$$

where $\rho_{\min}(\theta)$ denotes the shortest distance from the Hough origin to the line passing inside the circle given θ as shown in Fig. 3. For the easy calculation of $\rho_{\min}(\theta)$, the Hough origin is located at $(0, \nu_y)$ which moves along with previously detected vanishing point. Then, we have $\rho_{\min}(\theta) = \nu_x \sin\theta - \rho_{local}$. It should be emphasized that the upper and lower bounds of $\rho(\theta)$ varies according to θ, but the size of the range remains constant regardless of θ as

$$|\rho(\theta)| = 2\rho_{local} \tag{3}$$

and thus the total memory size is reduced to $\lceil 2\rho_{local}/q_\rho \rceil \times \lceil \pi/q_\theta \rceil$ which is less than conventional one by $2\rho_{local}/\rho_{max}$ times.

For the intuitive understanding of the proposed memory reduction method, we give an example as shown in Fig. 4. As can be seen in Fig. 4(a), the conventional method requires the overall accumulation array, but the proposed method in Fig. 4(b) uses much smaller array which is defined by the region inbetween green (lower bound, $\rho_{\min}(\theta)$) and blue (upper bound, $\rho_{\min}(\theta) + 2\rho_{local}$) curves in Fig. 4(a).

C. Modified Parametric Domain

The proposed method performs tracking on the parametric domain to consider the temporal coherency. The temporal coherency in the lane detection implies that a variation of lateral position of lane is small between two captured images because a lateral movement of vehicle is slow. Hence the current lateral position of the lane can be searched in the vicinity of the previously detected position by the temporal coherency. For this we propose a modified parametric domain by introducing a new parameter ϖ which encodes the lateral

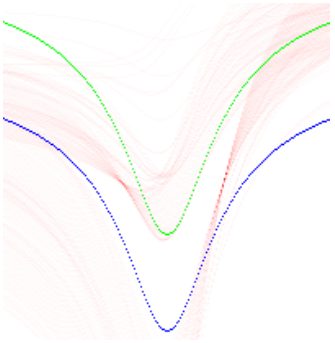

(a) conventional

(b) proposed

Fig. 4. Snap shots of the accumulation array where x-axis is for θ and y-axis for ρ

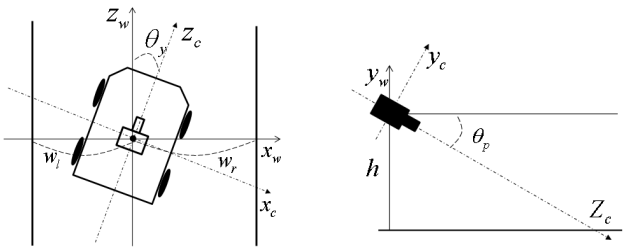

(a) (b)

Fig. 5. Five extrinsic parameters and two coordinates (arrows for world coordinate $\mathbf{X_w} = (x_w, y_w, , z_w)$ and dotted arrows for camera coordinate $\mathbf{X_c} = (x_c, y_c, z_c)$). (a) Top view. Yaw angle (θ_y) and lateral positions (w_l, w_r) are shown. (b) Lateral view. Height (h) and pitch angle (θ_p) are shown.

position of the lane. Note that the purpose of proposing the modified parametric domain is not to estimate accurate lateral positions but to encode information about lateral positions for the tracking on the parametric domain. Hence approximated lateral positions are encoded in the parameter ϖ ,which will be obvious later.

To begin with, a world coordinate $\mathbf{X_w} = (x_w, y_w, z_w)$ is related to an image coordinate $\mathbf{X} = (X, Y)$ given extrinsic and intrinsic parameters [12]. First, the extrinsic parameters determine a position of camera relative to road plane and relate the world coordinate $\mathbf{X_w}$ to the camera coordinate $\mathbf{X_c} = (x_c, y_c, z_c)$. Note that two coordinates are depicted in Fig. 5 by arrows for the world coordinate and dotted arrows for the camera coordinate. There are five extrinsic parameters : pitch angle (θ_p) between road plane and camera orientation, yaw angle (θ_y) between driving direction and camera orientation, lateral positions (w_l, w_r) from optical center of camera to a lane and height (h) from ground to the optical center of camera as shown in Fig. 5. With the extrinsic parameters, the camera coordinate $\mathbf{X_c}$ is related to the world coordinate $\mathbf{X_w}$ by

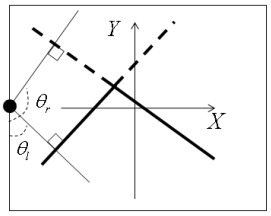

Fig. 6. Two lanes on image coordinate $\mathbf{X} = (X, Y)$. Thick lines represents projected left and right lanes to the image plane and they are dotted above the vanishing point. Two lines are related to the hough angles θ_l and θ_r.

$$\mathbf{X_w} = \mathcal{R}\mathbf{X_c} + \mathcal{T} \tag{4}$$

where

$$\mathcal{R} = \begin{bmatrix} 1 & 0 & 0 \\ 0 & \cos\theta_p & \sin\theta_p \\ 0 & -\sin\theta_p & \cos\theta_p \end{bmatrix} \begin{bmatrix} \cos\theta_y & 0 & \sin\theta_y \\ 0 & 1 & 0 \\ -\sin\theta_y & 0 & \cos\theta_y \end{bmatrix},$$
$$\mathcal{T} = \begin{bmatrix} 0 & h & 0 \end{bmatrix}^T.$$

Next, the intrinsic parameters relate the camera coordinate $\mathbf{X_c}$ to an image coordinate $\mathbf{X} = (X, Y)$ in Fig. 6 by

$$\begin{aligned} X &= \frac{f}{k}\frac{x_c}{z_c} \\ Y &= \frac{f}{l}\frac{y_c}{z_c} \end{aligned} \tag{5}$$

where f means a distance from lens to CCD and k (l) means width (height) of a cell in CCD. Based on (4) and (5) two parallel lanes $x_w = w_1$, $x_w = w_2$ on the world coordinate system are projected to the image coordinate system as shown in Fig. 6 where the lanes are represented by thick lines and it is not difficult to show that two line equations on the image coordinate system are given by

$$\begin{aligned} Y = &-(\frac{h}{w_l}\cos\theta_y - \sin\theta_y\sin\theta_p)\frac{X}{\cos\theta_p} \\ &-(\frac{h}{w_l}\sin\theta_y + \cos\theta_y\sin\theta_p)\frac{f}{\cos\theta_p} \\ Y = &-(\frac{h}{w_r}\cos\theta_y - \sin\theta_y\sin\theta_p)\frac{X}{\cos\theta_p} \\ &-(\frac{h}{w_r}\sin\theta_y + \cos\theta_y\sin\theta_p)\frac{f}{\cos\theta_p}. \end{aligned} \tag{6}$$

Then the lines are related to hough angles θ_l and θ_r, and the relationship between the slope and the hough angle is expressed by

$$\begin{aligned} \tan\theta_l &= -(\frac{h}{w_l}\cos\theta_y - \sin\theta_y\sin\theta_p)\frac{1}{\cos\theta_p} \\ \tan\theta_r &= -(\frac{h}{w_r}\cos\theta_y - \sin\theta_y\sin\theta_p)\frac{1}{\cos\theta_p}. \end{aligned} \tag{7}$$

Since $\theta_p \approx 0$ when the camera is mounted on the car (if it is not the case, we can mount the camera so that $\theta_p \approx 0$), trigonometric functions can be approximated by $\cos\theta_p \approx 1$ and $\sin\theta_p \approx \theta_p$. Also under the assumption that $\frac{h}{w_l}\cos\theta_y \gg \sin\theta_y\theta_p$, (7) can finally be written by

$$\begin{aligned} w_l &\approx \kappa(\theta_y)\cot\theta_l \\ w_r &\approx \kappa(\theta_y)\cot\theta_r, \end{aligned} \tag{8}$$

where $\kappa(\theta_y) = -h\cos\theta_y$. As can be seen in (8), $\cot\theta_l$ and $\cot\theta_r$ are related to the lateral positions w_l and w_r respectively, and thus we define new parameter ϖ to encode the lateral position by

$$\varpi = \cot\theta. \tag{9}$$

As a result, we have $\rho - \varpi$ domain based on (9) instead of conventional $\rho - \theta$ domain.

D. Proposed Lane Detection System

In this section, we combine results of above three subsections to complete the lane detection system. In our system, an accumulation array is first prepared for ρ-ϖ domain. Although $\cot\theta$ goes to infinite as θ approaches 0 and thus ϖ is not delimited, we can define reasonable range of $\cot\theta$ depending on camera geometry because projected lanes to an image are not severely inclined toward horizontal line. With this observation, let us assume that $|\varpi| \leq \tau$. Then according to Section III-B, the size of the accumulation array becomes $\lceil 2\rho_{local}/q_\rho \rceil \times \lceil 2\tau/q_\varpi \rceil$ where q_ϖ is a quantization step of ϖ. Given the accumulation array, each extracted ridge point $\mathbf{x}_i = (x_i, y_i)$ from the Section III-A is converted to the modified parametric domain by

$$\rho = \mathcal{C}(\varpi)x_i + \mathcal{S}(\varpi)y_i - \varrho_{min}(\varpi) \tag{10}$$

where $\mathcal{C}(\varpi) = \cos\theta = \varpi/\sqrt{1+\varpi^2}$, $\mathcal{S}(\varpi) = \sin\theta = 1/\sqrt{1+\varpi^2}$ and $\varrho_{\min}(\varpi) = \rho_{\min}(\theta) = \nu_x/\sqrt{1+\varpi^2} - \rho_{local}$, and corresponding cells are incremented by 1. When implementing this accumulation procedure in fixed point, we can set up lookup table for $\mathcal{C}(\varpi)$, $\mathcal{S}(\varpi)$ and $\varrho_{\min}(\varpi)$ without explicitly calculating them. Note that only cells that satisfy $0 \leq \rho \leq 2\rho_{local}$ are processed in our method, that is, the cells outside the region inbetween blue curve and green curve in Fig. 4(a) are not processed and it gives another computational savings.

After completing the accumulation for all the ridge points, current left lane $\Lambda_L^c = (\rho_L^c, \varpi_L^c)$ and right lane $\Lambda_R^c = (\rho_R^c, \varpi_R^c)$ are detected by searching maximally voted cells in the accumulation array. However false detection may occur when we work with current image alone because spurious lines would predominantly present. Hence we consider temporal coherency by searching current lanes Λ_L^c, Λ_R^c on the modified parametric domain in the vicinity of the previous lanes Λ_L^p and Λ_R^p. More formally in the case of detecting the left lane, search range is defined by a rectangular window Ω ($[\rho_L^p - \tau_\rho, \rho_L^p + \tau_\rho] \times [\varpi_L^p - \tau_\varpi, \varpi_L^p + \tau_\varpi]$) where τ_ρ and τ_ϖ determines the window size, and then maximally voted cell is searched in Ω. The right lane detection is processed in the same manner. Note that initial lateral positions are detected by finding maximally voted cells on the left plane of ROIPD $[0, 2\rho_{local}] \times [-\tau, 0]$ for the left lane and the right plane of

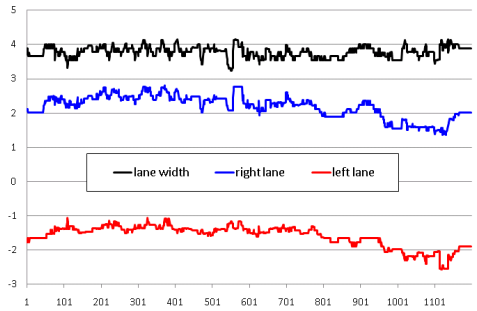

Fig. 7. The measured lateral positions and lane width on the video sequence of 1200 frames.

TABLE I
AN EXAMPLE OF PARAMETER SETTING

parameter	parameter description	value
T_s	ridge saliency threshold	10
T_c	ridge scale threshold	13
τ	range of ϖ	4
q_ϖ	quantization step of ϖ	0.08
$2\rho_{local}$	range of ρ	28
q_ρ	quantization step of ρ	1
τ_ρ	search range of ρ	5
τ_ϖ	search range of ϖ	5

ROIPD $[0, 2\rho_{local}] \times [0, \tau]$ for the right lane, and applying strong threshold to the counts corresponding to the detected cells.

Let us denote slopes of the detected left and right lanes in the image coordinate depicted in Fig. 6 as a_l and a_r respectively, and intercepts as b_l and b_r respectively. Comparing these values with those in linear equations in (6), several algebraic steps give estimates of the left and right lateral positions, $\tilde{w}_l$ and $\tilde{w}_r$ as follows :

$$\begin{aligned} \tilde{w}_l &= \frac{h\cos\theta_y}{\sin\theta_y \sin\theta_p - a_l \cos\theta_p} \\ \tilde{w}_r &= \frac{h\cos\theta_y}{\sin\theta_y \sin\theta_p - a_r \cos\theta_p}, \end{aligned} \tag{11}$$

where $\theta_y = \arctan(\frac{b_l - b_r}{a_l - a_r}\frac{1}{f})$ and $\theta_p = \arctan(a_l \sin\theta_y - b_l \cos\theta_y \frac{1}{f})$. To verify the accuracy of the estimates in (11), the lane width is calculated by $\tilde{w}_r - \tilde{w}_l$ and its variance is measured. The reason why the variance of the lane width is chosen as a verification quantity for the accuracy of the estimates of lateral positions is that the lane width remains nearly constant. The lateral positions and corresponding lane width measured on the video sequence of 1200 frames are depicted in Fig. 7 and we found that mean value is $3.777m$ and variance is 0.0273. We believe that this value of variance is acceptable.

IV. EXPERIMENTAL RESULTS

For the experiments, we implemented the proposed system on both DSP (TI TMS320DM6435, 400MHz) and PC. In DSP implementation, we found that execution speed is around 30fps for 352×240 video sequence and the proposed method is shown to be fast and memory efficient. To visually show the result of the proposed method, exactly same code is implemented on PC, and two scenarios, lane changing case and curved lane case are captured and depicted in Fig. 8 and Fig. 9. In whole experiments, parameters are set as in TABLE 1. Note that the size of the proposed accumulation array is just 100 × 28 ($\lceil 2\tau/q_\varpi \rceil \times \lceil 2\rho_{local}/q_\rho \rceil$) according to TABLE I, which is just 7.5% of the conventional one.

First in the lane changing case of Fig. 8(a) which captures the moment when the lane is exactly located on the center of a vehicle (camera optical center), almost the ridges are well extracted on the lane as shown in Fig. 8(b) and three dominant lanes are seen in the accumulation array of Fig. 8(c) where green and blue points represent previously detected lane and current lane respectively and faint blue represents search region. Since our method performs tracking on the parametric domain, we can continuously detect the lane even when the vehicle is changing the lane. The detected lanes are depicted in Fig. 8(d) where green lines represent detected lanes, red circle represents a current vanishing point and red circle represents a range where the next vanishing point would be found. It should be noted that the search region Ω is defined as a rectangular window in subsection III-D, but Ω in Fig. 8(c) appears to be skewed and elongated because $\varrho_{min}(\varpi)$ in (10) causes a non-homogeneous bias. Second, curved lane case is shown in Fig. 9. In spite of the curved lane, the lane appears to be straight in the near field and the extracted ridges in the near field are seen as collinear as shown in Fig. 9(b). Hence the lines corresponding to maximally voted cells in the accumulation array of Fig. 9(c) are well localized on real lanes as shown in Fig. 9(d).

V. CONCLUSIONS

In this paper, we have presented fast lane detection & tracking method based on Hough transform. By confining the region of lane search based on the previously detected vanishing point, the size of the accumulation array is greatly reduced and thus the computations are reduced. In addition, tracking scheme on the parametric domain well incorporates temporal coherency and enables to robustly detect the lane even when the lane is weakly represented on the parametric domain. From the result of DSP implementation, the proposed method is also shown to be adequate for practical system.

VI. ACKNOWLEDGEMENT

This research was supported by Basic Science Research Program through the National Research Foundation of (NRF) funded by the Ministry of Education, Science and Technology (2009-0083495)

REFERENCES

[1] R. Okada, Y. Taniguchi, K. Furukawa, and K. Onoguchi, "Obstacle detection using projective invariant and vanishing lines," in *IEEE International Conference on Computer Vision*, vol. 1, Oct. 2003, pp. 330–337.

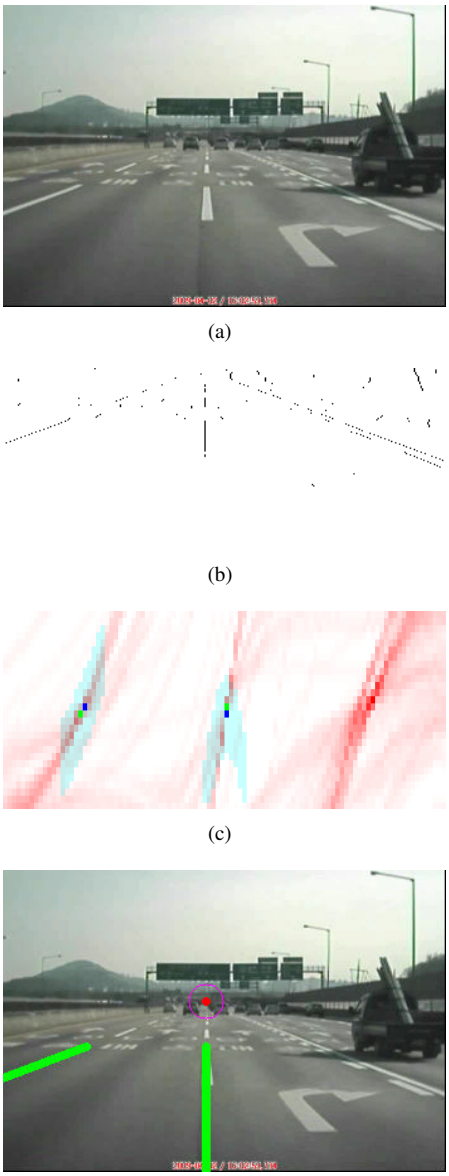

(a) (b) (c) (d)

Fig. 8. Simulation results. (a) Input image (b) Extracted ridges (c) Snap shot of an accumulation array (d) Detected Lanes

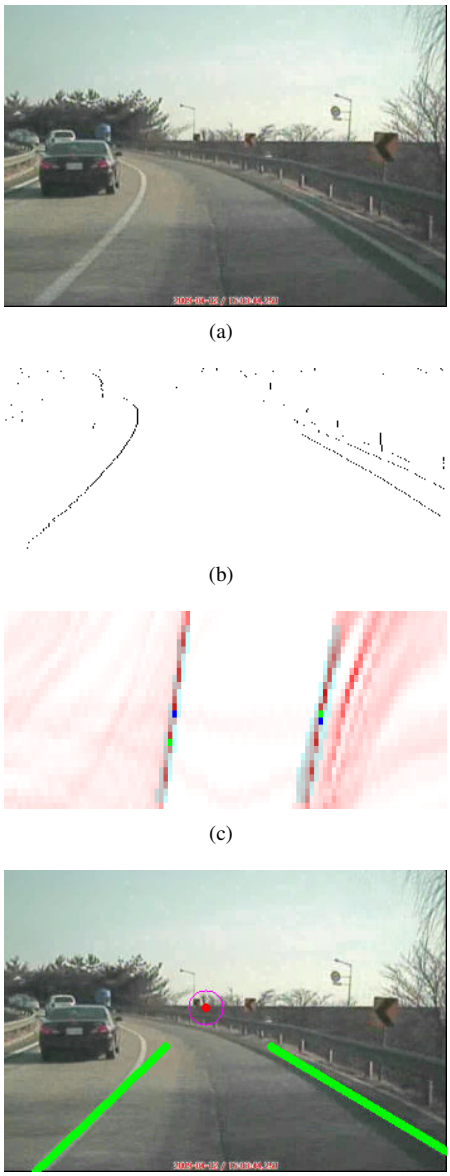

(a) (b) (c) (d)

Fig. 9. Simulation results. (a) Input image (b) Extracted ridges (c) Snap shot of an accumulation array (d) Detected Lanes

[2] D. Schreiber, B. Alefs, and M. Clabian, "Single camera lane detection and tracking," in *IEEE International Conference on Intelligent Transportation Systems*, Sept. 2005, pp. 302–307.

[3] J. Kaszubiak, M. Tornow, R. Kuhn, B. Michaelis, and C. Knoeppel, "Real-time vehicle and lane detection with embedded hardware," in *IEEE Proceedings of Intelligent Vehicles Symposium*, June 2005, pp. 619–624.

[4] A. Saudi, J. Teo, M. H. A. Hijazi, and J. Sulaiman, "Fast lane detection with randomized hough transform," in *International Symposium on Information Technology*, vol. 4, Aug. 2008, pp. 1–5.

[5] H. Wang and Q. Chen, "Real-time lane detection in various conditions and night cases," in *IEEE International Conference on Intelligent Transportation Systems*, Sept. 2006, pp. 1226–1231.

[6] Z. Kim, "Robust lane detection and tracking in challenging scenarios," *IEEE Transactions on Intelligent Transportation Systems*, vol. 9, no. 1, pp. 16–26, March 2008.

[7] R. Labayrade, J. Douret, and D. Aubert, "A multi-model lane detector that handles road singularities," in *IEEE conference on Intelligent Transportation Systems*, Sept. 2006, pp. 1143–1148.

[8] B. Southall and C. Taylor, "Stochastic road shape estimation," in *IEEE International Conference on Computer Vision*, vol. 1, 2001, pp. 205–212.

[9] R. F. Frangi, W. J. Niessen, K. L. Vincken, and M. A. Viergever, "Multiscale vessel enhancement filtering." Springer-Verlag, 1998, pp. 130–137.

[10] M. Jacob and M. Unser, "Design of steerable filters for feature detection using canny-like criteria," *IEEE Trans. Pattern Anal. Mach. Intell*, vol. 26, pp. 1007–1019, 2004.

[11] J. McCall and M. Trivedi, "Video-based lane estimation and tracking for driver assistance: survey, system, and evaluation," *IEEE Transactions on Intelligent Transportation Systems*, vol. 7, no. 1, pp. 20–37, March 2006.

[12] D. A. Forsyth and J. Ponce, *Computer Vision: A Modern Approach*. Prentice Hall, August 2002.